Chaos-assisted tunnelling in the absence of reflexion symmetry

1998 J. Phys. A: Math. Gen. 31 9469

(http://iopscience.iop.org/0305-4470/31/47/008)

J. Phys. A: Math. Gen. **31** (1998) 9469–9481. Printed in the UK PII: S0305-4470(98)95962-5

Chaos-assisted tunnelling in the absence of reflexion symmetry

Steven Tomsovic

Department of Physics, Washington State University, Pullman, WA 99164-2814, USA

Received 15 July 1998

Abstract. It has been shown previously that a novel tunnelling behaviour, dubbed chaos-assisted tunnelling, can arise in bound, mixed phase space systems possessing reflection symmetries. As with the usual, direct tunnelling problem of a double well, even a very weak symmetry breaking typically quenches the ability of certain probability densities to tunnel resonantly back and forth. Experiments lacking exact reflexion symmetry will fail to exhibit tunnelling. We show here how chaos-assisted tunnelling can be re-established experimentally and distinguished from direct tunnelling through the variation of two external system parameters, and demonstrate the applicability of a generalized three-level model of the tunnelling process with the coupled quartic oscillators.

1. Introduction

Fundamental differences arise in the behaviour of tunnelling in one-degree-of-freedom autonomous systems versus more-degree-of-freedom systems. Just as the extra degrees of freedom engender the possibility of far more complicated system dynamics, these additional dynamical behaviours may underlie new possible features of tunnelling. Recent studies in simple dynamical systems possessing more than a single degree of freedom have led to a number of newly identified phenomena. Some examples are found in chaos-assisted tunnelling [1, 2], tunnelling behaviours between chaotic eigenstates [3], tunnelling between strongly localized states [4], chaos-assisted ionization [5], and the properties of light emission from lasing resonant cavities [6].

Our primary concern in this paper is chaos-assisted tunnelling and broken (or non-existant) symmetry. This tunnelling is dynamical in nature and, in fact, no potential barrier need exist at all. As conceptualized up to now [1], for chaos-assisted tunnelling to exist the system should have discrete symmetries, and the underlying dynamics contain a mixture of regular and globalized chaotic motion. The regular regions in phase space are marked by the existence of a dense set of tori on which the system undergoes quasiperiodic motion, and the rest is filled by a chaotic sea. It is typical for tori in mixed phase space systems to have lower symmetry than the full system. Rather it is far more exceptional for a torus to map into itself under all the symmetry operations. Those tori which have a lower symmetry must be replicated exactly elsewhere in phase space leading to the expectation of degeneracies via semiclassical theory. The tunnelling occurs between wavefunctions localized to (semiclassically quantized on) congruent, but distinct tori [7]. A direct tunnelling mechanism would be characterized by the localized states being coupled but isolated from the rest of the levels. In contrast, chaos-assisted tunnelling splittings are

0305-4470/98/479469+13$19.50

governed by weak coupling of one or more of the localized states to irregular eigenstates associated with the chaotic region in the phase space, but without direct coupling amongst the localized levels. The resultant splittings are extremely sensitive to variation of any external parameter that shifts the irregular spectrum. The splittings can fluctuate orders of magnitude, and there is no simple theoretical form for them depending on an exponential of $\overline{h}^{-1}$.

Very weak symmetry breaking is capable of quenching the tunnelling. This is especially true at higher excitation energies if the tunnelling is dynamical. In this case the tunnelling splittings typically decrease with increasing excitation energy where the system is 'more semiclassical'. If the discrete symmetries of a system are not fundamental, but rather a virtue of design, it may be effectively impossible to impose the symmetry well enough to maintain resonant tunnelling. The lack of exact symmetry applies to many conceivable experiments in quantum dots, and microwave, optical, and acoustic cavities where weak disorder or machining imprecision are sufficient to prevent the resonant tunnelling behaviour. Such experiments are the primary motivation for the investigation discussed in this paper.

For illustration of symmetry-breaking effects with a simple barrier tunnelling example, one could change slightly the depth of one of the wells in the symmetric double well Hamiltonian and there would not be transfer of probability from one well to the other and back with time. However, if the relative well depths are smoothly changed further as a function of a parameter, tunnelling between certain pairs of states would occur for narrow ranges of parameter values nearby where the levels undergo an avoided crossing. The width of the parameter range where tunnelling takes place would be proportional to the splitting. This is the broken symmetry regime of interest here. Whereas even if there exists an extremely good symmetry, it is broken sufficiently by weak disorder or other small perturbations such that the tunnelling would be nil, and it is necessary to vary a parameter to tune the system through tunnelling regimes associated with avoided crossings in the spectrum—the smaller the splitting, the smaller the regime. This puts a very stringent requirement on any experimental attempt to see this tunnelling. There must be very stable and fine controls over the external parameters. Of course, it is not necessary to have an approximate symmetry at all. The avoided crossings between any two localized states will still generally be associated with dynamical tunnelling. The main question is thus, what are the essential features of chaos-assisted tunnelling under these circumstances and how experimentally could one re-establish tunnelling and distinguish it unambiguously from ordinary direct processes?

In the next section, we propose a three-level model incorporating two localized states and a single irregular state, generalized with respect to that given in [1] for the absence of symmetry, that captures the simplest tunnelling mechanism without reflexion symmetry. It turns out that it is necessary to vary two external parameters, one which tunes the system through crossings between localized levels and the other to displace the irregular levels near the crossing pair. In section 3, we give an example using the desymmetrized, coupled quartic oscillators. We end with a brief discussion of coupling to multiple irregular states and the conclusions.

2. Asymmetric three-level model

The simplest model begins with a three-dimensional subspace of the system spanned by two orthonormal states denoted $\{\Psi_L, \Psi_R\}$ imagined as being localized to tori (L for left and R for right—not to be taken literally), and another orthonormal irregular, delocalized state, Ψ_C (C for chaotic). In this subspace, the parameter-dependent Hamiltonian can be locally

expressed as

$$\hat{H}_3(\alpha,\lambda)\begin{pmatrix}\Psi_L\\ \Psi_R\\ \Psi_C\end{pmatrix}=\begin{pmatrix}-E(\alpha) & 0 & v_1\\ 0 & E(\alpha) & v_2\\ v_1 & v_2 & E_c(\lambda)\end{pmatrix}\begin{pmatrix}\Psi_L\\ \Psi_R\\ \Psi_C\end{pmatrix} \tag{1}$$

where the nul matrix element indicates that direct tunnelling is not occurring. If our goal were to study the competition between direct and chaos-assisted processes, we would incorporate a third parameter for this matrix element. The parameter α moves the system through a crossing of the two localized levels, and λ changes the proximity of the closest, coupled irregular state. In an actual system, the tunnelling matrix elements, $\{v_1, v_2\}$, vary very little over the small local $\{\alpha, \lambda\}$ domain over which avoided crossings occur and are therefore considered constants. However, they do differ from one realization of tunnelling in the system's full spectrum to another (i.e. from one neighbourhood of an avoided crossing between localized states to another) and various matrix element ratios, $r = |v_2/v_1|$, have to be considered. If there is a weakly broken reflection symmetry and the quantum numbers of Ψ_L and Ψ_R are the same, r would be expected to be very close to unity. Otherwise, v_1 and v_2 would be expected, *a priori*, to be independent. They would behave like random variables from one tunnelling triplet realization to another. If they varied in a Gaussian fashion as a simple random matrix model would suggest, the distribution of encountered values of r would be Lorentzian. Without loss of generality, $E(\alpha)$ and $E_C(\lambda)$ can be taken to depend linearly on α and λ respectively. Two simplifications would reduce this model to one appropriate for a symmetric system as given in [1]. The first is $E(\alpha) = 0$, eliminating the α parameter entirely. The second is that $|v_2| = |v_1|$. Thus by switching to a basis with a symmetrized and antisymmetrized combination of $\{\Psi_L, \Psi_R\}$, one of the two non-irregular basis states completely decouples from the problem. The consequences of that model follows exclusively from diagonalization of the 'active' two-by-two submatrix. Here the full three dimensions enter.

The first step is to determine the conditions required for tunnelling to take place in this system. Consider the evolving probability,

$$P(t) = |\langle\Psi_R|\exp(-\mathrm{i}\hat{H}t/\hbar)|\Psi_L\rangle|^2 \tag{2}$$

which measures the likelihood of being found on the right after initially being localized on the left. At some unspecified later time τ, $P(\tau)$ attains unity if the tunnelling is complete. Since this may not be the case, it is of interest to know the maximum possible transfer of probability, $\mathcal{P}$, from one localized state to the other. Expanding the localized states in terms of the eigenstates,

$$\begin{aligned}|\Psi_L\rangle &= \sum_{j=1}^{3} a_{Lj}|E_j\rangle\\ |\Psi_R\rangle &= \sum_{j=1}^{3} a_{Rj}|E_j\rangle\end{aligned} \tag{3}$$

one finds

$$\begin{aligned}P(t) &= |\langle\Psi_R|\mathrm{e}^{-\mathrm{i}\hat{H}t/\hbar}|\Psi_L\rangle|^2 = \left|\sum_{j=1}^{3} a_{Lj}a_{Rj}^{*}\mathrm{e}^{-\mathrm{i}E_jt/\hbar}\right|^2\\ \mathcal{P} &= \max\{P(t)\} = \left(\sum_{j=1}^{3}|a_{Lj}a_{Rj}^{*}|\right)^2\end{aligned} \tag{4}$$

where the $|E_j\rangle$ are the three true eigenstates of the three-level model. To understand the implications of equation (4), it is convenient to introduce symmetrized and antisymmetrized states built on $\{|\Psi_L\rangle, |\Psi_R\rangle\}$. For time-reversal invariant systems, complex phases are unnecessary, and

$$|\pm\rangle = \frac{1}{\sqrt{2}}|\Psi_L\rangle \pm \frac{1}{\sqrt{2}}|\Psi_R\rangle \tag{5}$$

if $\{|\Psi_L\rangle, |\Psi_R\rangle\}$ themselves are time-reversal invariant states. If the above expression for $\mathcal{P}$ is to attain unity, it turns out that one of the three eigenstates must be given by $|\pm\rangle$. To begin with, normalization constraints require that $|a_{Lj}|$ must equal $|a_{Rj}|$ for all j†. From orthogonality constraints, the signs cannot all be the same nor all different. But if only one of the signs is different, the antisymmetric linear combination reduces to an expansion of a single term, i.e. is an eigenstate. If two of the signs are different, the symmetric linear combination is an eigenstate. The other two eigenstates can be any linear combination of the remaining two, $|\mp\rangle$ and $|\Psi_C\rangle$. This is the three-level generalization of the usual, direct two-level result that the eigenstates have the form $|\pm\rangle$. Another form of the $\mathcal{P}$ relation follows by substituting $|\pm\rangle$ into the equation above which leads to

$$\begin{aligned} P(t) &= |\langle\Psi_R|\mathrm{e}^{-\mathrm{i}\hat{H}t/\hbar}|\Psi_L\rangle|^2 = \left(\tfrac{1}{2}\sum_{j=1}^{3}(|\langle E_j|+\rangle|^2 - |\langle E_j|-\rangle|^2)\mathrm{e}^{-\mathrm{i}E_j t/\hbar}\right)^2 \\ \mathcal{P} &= \max\{P(t)\} = \left(\tfrac{1}{2}\sum_{j=1}^{3}||\langle+|E_j\rangle|^2 - |\langle-|E_j\rangle|^2|\right)^2. \end{aligned} \tag{6}$$

Again keeping in mind orthonormality constraints, equation (6) is easily seen to be consistent with $\mathcal{P} = 1$ only if $|+\rangle$ or $|-\rangle$ is one of the eigenstates.

For almost all values of $\{\alpha, \lambda, r\}$, this condition is not met precisely; see figure 1. The maximum tunnelling probability is calculated for the above three-level model using two different matrix element ratios. It illustrates three main points: (i) the tunnelling shuts off if the unperturbed localized states are separated in energy further than v_2 no matter how close the chaotic level, (ii) the behaviour is distinct from the direct tunnelling case where there would be no λ-parameter dependence since the position of other levels relative to the tunnelling pair would be irrelevant, and (iii) the parameter domain of significant tunnelling shrinks as the matrix element ratio, r, gets further from unity.

The narrowing range of significant tunnelling with respect to α as the chaotic level moves further away betrays a second important distinction between chaos-assisted and direct tunnelling. The tunnelling time increases proportionally to the distance to the coupled chaotic level. More generally, this is the root of the splittings' sensitivity to external parameter variation mentioned in the first paragraph: for a statistical theory of the fluctuations see [8]. Perturbation theory suffices to understand the probability narrowing and increasing time effect. It also describes the natural regime in which the admixtures between Ψ_C and $\{\Psi_L, \Psi_R\}$ are very weak, i.e. $E_C \gg v_1, v_2, E(\alpha)$. Perturbative diagonalization of the coupling between the chaotic level and the localized levels leads to a second-order two-level system whose Hamiltonian is

$$\hat{H}_2(\alpha, \lambda)\begin{pmatrix}\Psi'_L\\ \Psi'_R\end{pmatrix} = \begin{pmatrix}-E(\alpha) - (\pm)v_t/r & -v_t\\ -v_t & E(\alpha) - (\pm)rv_t\end{pmatrix}\begin{pmatrix}\Psi'_L\\ \Psi'_R\end{pmatrix} \tag{7}$$

† Interestingly enough, if the system is not time reversal invariant, it is not necessary that one of the eigenstates be a generalized (complex coefficient) version of $|\pm\rangle$, and equation (6) does not hold. The normalization constraints still require that $|a_{Lj}| = |a_{Rj}|$ for all j.

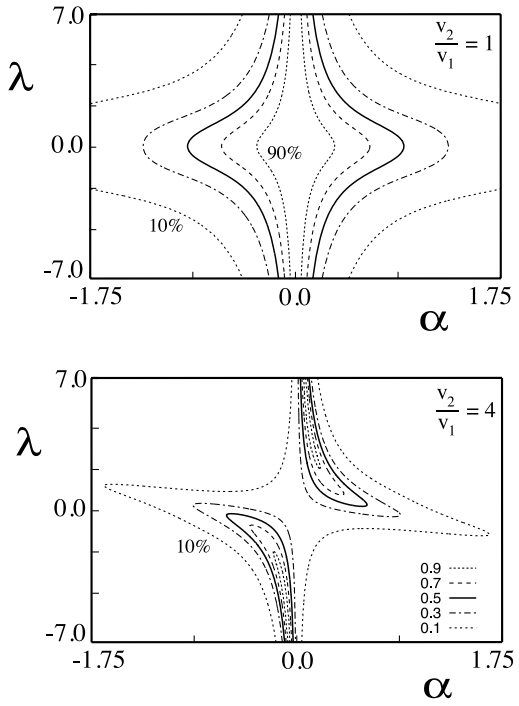

Figure 1. Contour plot of the maximum tunnelling probability, $\mathcal{P}$, versus the two parameters, $\{\alpha, \lambda\}$. In the upper figure, $r = |v_2/v_1| = 1$, and in the lower figure, $r = 4$. $E_l(\alpha)$ varies linearly with α over the interval $\{-1.75v_2, 1.75v_2\}$, i.e. $E_l(\alpha) = \alpha v_2$. E_C varies linearly with λ over the interval $\{-7v_2, 7v_2\}$, i.e. $E_C = \lambda v_2$. The (10%, 30%, 50%, 70%, 90%) tunnelling probability contours are drawn. The solid curves are the 50% tunnelling probability contours.

where $(\pm)$ is positive if $v_1 v_2 > 0$ and negative otherwise. There are two effects. One is an induced second-order tunnelling matrix element, v_t, directly connecting the two localized states

$$v_t = \frac{v_1 v_2}{E_C}. \tag{8}$$

This expression fixes a precise, non-trivial relationship amongst three avoided crossings. Each regular level crosses the path of the chaotic level as well as the tunnelling avoided crossing between the two localized states; see figure 3. The minimum energy gap of each, $\{\Delta E_t, \Delta E_1, \Delta E_2\}$, is approximately equal to the appropriate one of the set $\{2v_t, 2v_1, 2v_2\}$ to the extent that $\{v_1, v_2\}$ do not vary locally with $\{\alpha, \lambda\}$. In that case

$$\Delta E_t = \frac{\Delta E_1 \Delta E_2}{2E_C}. \tag{9}$$

Note that the minimum separation distance of the tunnelling pair's avoided crossing seen by varying α alone is larger if the chaotic level lies closer to the pair. Thus, one has explicitly the dependence of the tunnelling on the position of the chaotic level and the overlap of the localized states with the chaotic state.

The other effect is the repositioning of the two regular energy levels. If the first-order perturbation diagonalization leaves the energy levels closer than v_t, then tunnelling takes place. In cases where $r = 1$, the repositioning cancels, relatively speaking. Essentially, tunnelling takes place near $E(\alpha) = 0$ for a narrow α-interval proportional to v_t. For $r \neq 1$, the tunnelling is offset and occurs near $2E(\alpha) = (\pm)v_t(r - 1/r)$. At those points the perturbation has pushed the levels together, thus distorting the appearance of figure 1 relative to the $r = 1$ case. As the chaotic level moves further away, it becomes ineffective at pushing the localized levels together and the tunnelling probability slowly approaches the form of the $r = 1$ case. Finally, it follows from diagonalizing the projected Hamiltonian that

the time to tunnel resonantly from Ψ_l to Ψ_R and back is given by $\tau = \pi\overline{h}/|\Delta E| \approx |h/v_t|$ which has the linear growth with distance to the closest important chaotic level mentioned above. To summarize, the avoided crossing relation, the narrowing tunnelling probability range dependence, the tunnelling time dependence on E_C, and the existence of an orthogonal transformation from three eigenstates to two localized states and a chaotic level all serve to distinguish chaos-assisted from direct tunnelling processes.

3. Coupled quartic oscillator example

To illustrate the main features of interest, consider the coupled quartic oscillators; see [1] for an extensive background. The Hamiltonian we consider is given by

$$\hat{H}(\alpha, \lambda) = \frac{\boldsymbol{p}^2}{2} + a(\lambda)(q_1^4/b + bq_2^4 + \alpha q_1 q_2^3 + 2\lambda q_1^2 q_2^2). \tag{10}$$

Due to the homogeneous degree of the potential, the dynamics on any positive energy surface can be mapped onto any other. It suffices to study the $E = 1$ surface and scale the phase space coordinates appropriately for other energies. For example, the classical actions scale as $E^{3/4}$. $a(\lambda)$ is a constant chosen for calculational convenience, and because it simplifies the relation between the eigenvalues, E_n, at $\overline{h} = 1$ with the eigenvalues, $\overline{h}_n$, for which there is a solution at $E = 1$. That is $E_n^{-3/4}(\overline{h} = 1) = \overline{h}_n(E = 1)$. $b = \pi/4$ reduces the symmetry from that of a square to that of a rectangle. For $\alpha = 0$, and λ decreasing from 0 to -1, this system makes a transition from integrable dynamics through mixed phase space dynamics towards fully chaotic dynamics. It has been previously shown to exhibit chaos-assisted tunnelling over the range $\lambda \in [-0.50, -0.20]$ where there exists a mixed phase space dynamics consisting of a single dominant chaotic region and several islands of stable motion embedded within. The system is symmetric with respect to time reversal and separately, inversion with respect to q_1 and q_2. With $\alpha \neq 0$, a reflection symmetry remains along with time-reversal symmetry. However, if a localized state is being constructed on a torus possessing both these symmetries, it will not have multiple copies in phase space. Therefore, no quasidegeneracies are implied, and enough symmetry is broken for the purposes of this study.

The most significant stable islands in the relevant λ range correspond to motion along the diagonals. In figure 2, two such tori are shown projected into configuration space for the symmetric case ($\alpha = 0$). Locally changing the parameters $\{\alpha, \lambda\}$ in the potential deforms them, but they remain intact. As α increases from zero, the equipotential contour moves as indicated by the marked arrows. A localized state constructed on a torus which is being 'stretched' moves down through the spectrum with the maximum slope locally (wavelength increasing), and one constructed on a torus being 'squeezed' moves up (wavelength decreasing). Regular states will show up in the spectrum as doublets that split significantly with increasing α forming the appearance of a sideways V. Figure 3 shows a portion of the spectrum. The localized states are readily visible (i.e. they follow the arrows). On the other hand, α has little influence on states, such as chaotic ones, which are excluded from motion along the diagonals. Such states move rather flatly across the spectrum with α (also readily visible). Although we can identify states localized along the configuration space diagonal solely from their level motions with respect to α, we have taken advantage of previous work which identified all the quantizing tori, their scaled actions, and quantum numbers. In this way, we will give results below for both quantizing tori and quantizing 'cantori' [9].

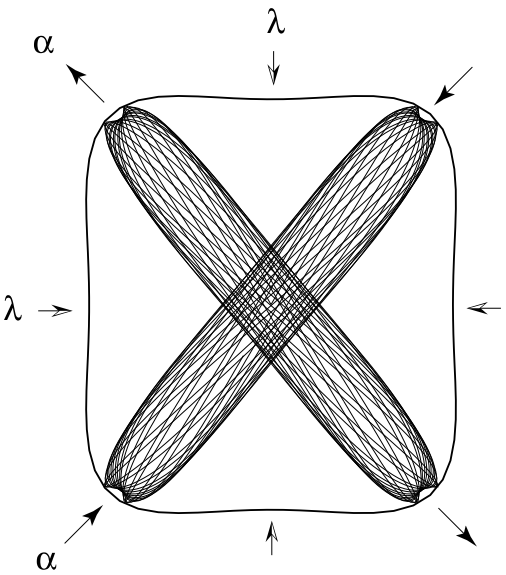

Figure 2. Two quasiperiodic classical trajectories (tori) of the Hamiltonian of equation (10) with $\{\alpha, \lambda\} = \{0.0, -0.25\}$; taken and modified from [1]. The equipotential encircles the trajectories. The arrows point to positions of maximum change in the equipotential by $\{\alpha, \lambda\}$ respectively. The full arrowheads indicate that α 'stretches' one torus whereas it 'compresses' the other. The half-filled arrowheads indicate the squeezing effect of λ on the chaotic eigenstates.

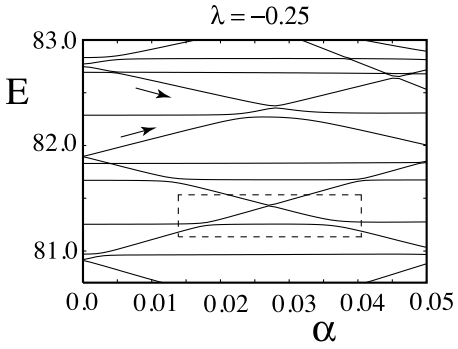

Figure 3. An excited-energy window in the coupled quartic oscillators' spectrum is shown for fixed λ as a function of the symmetry-breaking parameter α. The arrows indicate the slopes of a couple of the visible regular levels. The broken-line box encloses a very narrow tunnelling avoided crossing between two localized states in its upper centre. The tunnelling matrix elements connecting to the closest chaotic state, $\{v_1, v_2\}$ can be deduced from the two avoided crossings near the two lower corners. The tunnelling takes place only over a very tiny range of α near 0.0275.

Another feature seen in figure 2 is that λ alters the potential in a way that strongly affects the chaotic states' positions relative to localized states since the latter are insensitive to squeezing near the $q_1 = 0$ and $q_2 = 0$ lines. Thus, although in the coupled quartic oscillators $\{\alpha, \lambda\}$ do not have precisely the same meaning as in the three-level model, they are nearly identical and hence our use of the same notation. Note that a slight linear transformation to new variables $\{\alpha', \lambda'\}$ could be made to give a precise analogy to the three-level model parameters. In principle, this transformation is not global and must be determined separately for each quartic oscillator triplet of levels. In an experiment where one is varying parameters such as external field strengths, temperature, applied stresses etc, it may be unknown at the outset what effects the parameter variations are going to have on the levels. This poses no fundamental difficulty as long as the two parameter variations in question do not move the levels in a linearly dependent way. By measuring the effects of the two parameters, one can readily deduce the necessary linear transformation that isolates the parameter governing the localized states' avoided crossing from the parameter which changes the local spectrum of chaotic states. To an excellent approximation supposing the chaotic level not too close, one could fit the differences of the localized levels' energies with a linear function of $\{\alpha, \lambda\}$ and set it proportional to α'. To finish one would fit the energy difference between the mean position of the localized levels and the chaotic level to another linear function of $\{\alpha, \lambda\}$ and set it proportional to λ'. Together, these two equations

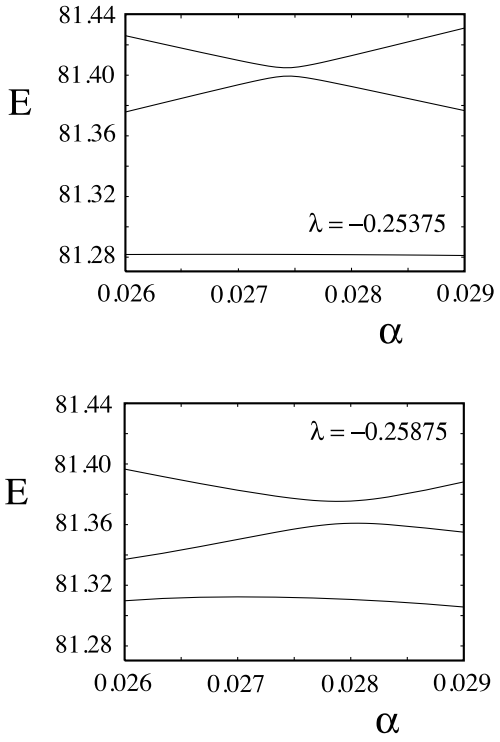

Figure 4. Expanded view of the level triplet inside the broken-line box of figure 3 for two different values of λ. As λ decreases, the chaotic level approaches the localized pair and has the effect of increasing the width of the avoided crossing. The width controls the tunnelling time and the range over which tunnelling can occur (it occurs roughly over the interval in which the localized states are within $\pm\sqrt{2}$ times the minimum energy separation).

would be sufficient if one needed the inverse transformation as well.

Reconstructing the equivalent of figure 1 for the quartic oscillators or, more generally any physical system, is a prohibitive amount of work. We therefore look for the other characteristic features of the three-level model. It already requires a certain amount of exploration to determine how broad a parameter range is necessary for the purposes of: (i) locating appropriate triplets—some localized avoided crossings may couple to two or more chaotic levels, (ii) covering the full avoided crossing of the pair of localized states, and (iii) varying the most important chaotic level from nearby to further away. For example, the broken-line box in figure 3 encloses one tunnelling example near $\alpha = 0.0275$. However, over the vast majority of α values, these levels are not involved in any tunnelling process.

We begin by verifying the applicability of the avoided crossing relation, equation (9). In figure 4, the triplet of levels shown is an expanded view from the previous figure (except that λ has been slightly shifted in value). In the upper half of the figure, significant tunnelling occurs only over the rather narrow range $\alpha \in [0.0272, 0.0277]$. For this specific case, it happens that the coupling matrix elements are $\{v_1, v_2\} = \{0.014, 0.026\}$, respectively, making the ratio $r = 1.86$; they are deduced by reconstructing the two chaotic-level-localized-level avoided crossings nearby. The localized pair of states undergoes a crossing whose minimum separation distance is inversely proportional to the distance of the chaotic level. By changing λ from -0.2525 to -0.2575, the chaotic level approached the tunnelling pair sufficiently to increase the minimum energy gap at the crossing from 0.0027 to 0.0073. The predicted gaps from equation (9) are respectively 0.0030 and 0.0064. Considering the assumptions of there being only one coupled chaotic level and the constancy of $\{v_1, v_2\}$, the use of perturbation theory, and the fact that one of the localized states is a cantorus quantizing well outside the boundary of the classical KAM island of regular motion, the agreement is

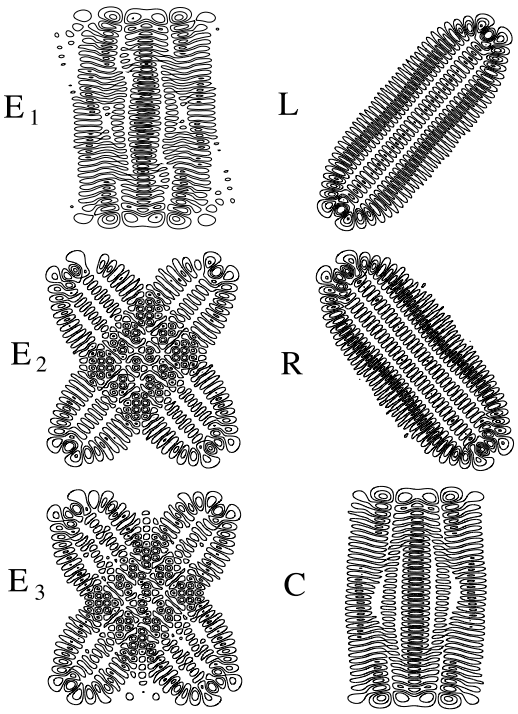

Figure 5. Quartic oscillator eigenstates and rotated wavefunctions. Three consecutive eigenstates and wavefunctions formed by nearly orthogonal linear combination are pictured for a constant set of contour levels. They are given for the three levels pictured in the upper part of figure 4 at the α-value (0.02743) leading to the minimum splitting between the localized states' eigenvalues. The linear combination is calculated to maximize the localization of $\{\Psi_L, \Psi_R\}$ and maximize the orthogonality of Ψ_C to them within the space defined by the three eigenstates.

quite good. In a second example that we have calculated at $E = 94.93$ involving quantizing bona fide tori, the results are even better, the predicted value is 0.00074 versus the actual 0.00076.

Next, to illustrate that tunnelling is taking place between two localized levels as claimed and that the chaotic level plays an important role, we consider the three correlation functions (final state either Ψ_L, Ψ_R, or Ψ_C) of the same form as the evolving tunnelling probability of equation (2). A straightforward method to making the needed calculations begins by seeking the optimal linear combinations of the three most important eigenstates needed to construct $\{\Psi_L, \Psi_R, \Psi_C\}$. To the extent that localized states are well represented in this way, it suffices. Otherwise coupling to more than one chaotic level is implied, and it is necessary to construct the EBK approximation directly and propagate the wavefunctions. In figures 5 and 6 we show two examples. The left column contains contour plots of the three eigenvectors nearest the tunnelling avoided crossing shown in the upper half of figure 4, and the right column shows the best $\{\Psi_L, \Psi_R, \Psi_C\}$-decomposition. Figure 5 corresponds to the first example discussed above where one of the localized states is quantized on a cantorus. It is distinguished by having three diagonal nodal lines. The other localized state lies just on the KAM island-chaos boundary. At this level of pictorial representation, there is no salient feature which distinguishes the quantized cantorus from a proper quantized torus. However, $\{\Psi_L, \Psi_R, \Psi_C\}$ deviate from orthogonality at the level of a percent or two. Figure 6 corresponds to the latter example at $E = 94.93$ and both localized states are quantized on tori well within the diagonal stable island boundaries. They are orthogonal to a part in 10^4. Note that: (i) the tunnelling in both these examples occurs between levels with differing quantum numbers, (ii) the three-level restriction causes no difficulty whatsoever in obtaining two highly localized three-level model states, $\{\Psi_L, \Psi_R\}$, whose correspondence to motion of the kind pictured in figure 2 is manifest: these states would match precisely to a direct

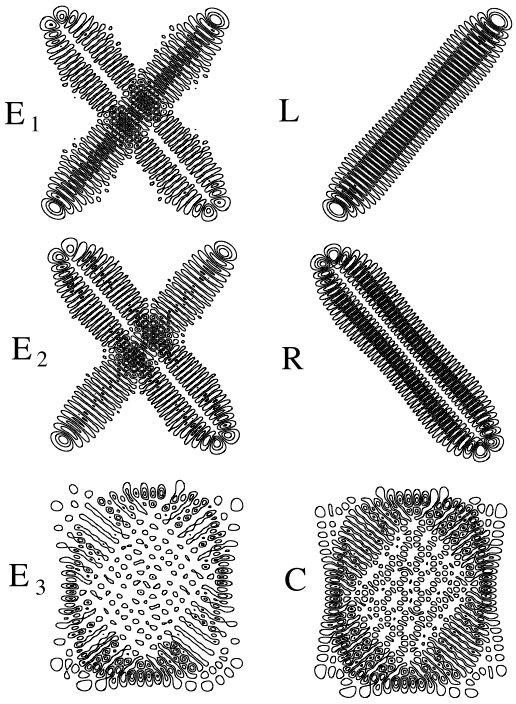

Figure 6. Quartic oscillator eigenstates and rotated wave functions. Similar to figure 5 except near energy $E = 94.93$, $\lambda = -0.2500$, and $\alpha = 0.023\,009$.

construction based on a semiclassical EBK-like approach, and (iii) the chaotic states are each localized to a great degree on known, short, unstable periodic orbits, i.e. a self-retracing vertical bouncing motion, and an oval path, respectively. *A priori*, this last point should be considered as being an accidental consequence of our selection of tunnelling examples. Not all chaotic states have to be so localized on short, unstable periodic orbits. If there is more to this 'accident', more investigation would be required to expose the reasons. Clearly, the larger the part of the Hilbert space associated with torus and cantorus quantization, the more constrained the set of possibilities for the remaining, chaotic states. They could, for example, be associated with a narrow band of phase space surrounding these unstable periodic orbits stretching part of the way along each one's stable and unstable manifolds because that is all the phase space remaining. We leave this question for another study.

In the tunnelling cases shown, over long times the evolution of a state initially localized on one diagonal moves completely over to the other (>95%). It will continue to move back and forth with time. The tunnelling correlation functions corresponding to figures 5 and 6 are pictured in figures 7 and 8. The time to tunnel from one localized state to the other is the low frequency oscillation visible. The superposed, high frequency oscillation reflects the role of the chaotic level in aiding the tunnelling process as discussed in [1]. The process is one of small amplitude transfer to the chaotic state that then transfers to the other localized state bit by bit. At no time is there a build-up of large probability on the chaotic state. The ratio of the tunnelling times of the two figures roughly equals the inverse ratio of the high-frequency oscillation amplitudes seen in the lower graphs, as predicted.

Still within the perturbative regime, the generalization of the three-level model to incorporate coupling to many chaotic levels is straightforward. In fact, equation (7) becomes

$$\hat{H}_2(\alpha,\lambda)\begin{pmatrix}\Psi'_L\\ \Psi'_R\end{pmatrix}=\begin{pmatrix}-E(\alpha)-\sum_i(\pm)_i\frac{v_{t,i}}{r_i} & -\sum_i v_{t,i}\\ -\sum_i v_{t,i} & E(\alpha)-\sum_i(\pm)_i r_i v_{t,i}\end{pmatrix}\begin{pmatrix}\Psi'_L\\ \Psi'_R\end{pmatrix} \tag{11}$$

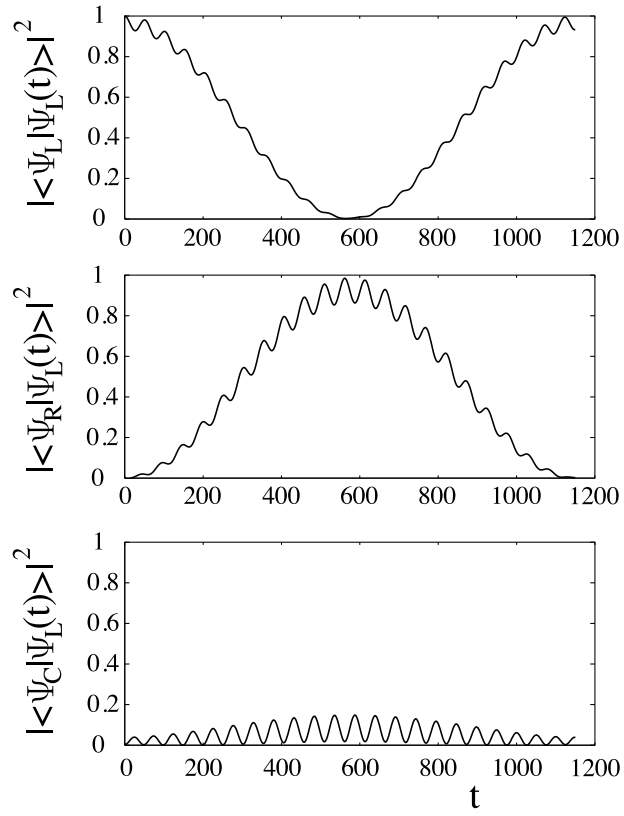

Figure 7. Time correlation functions of Ψ_L from figure 5.

where the index i is introduced to sum over the coupling to each of the chaotic levels. Tunnelling still takes place at the avoided crossing, and varying λ continues to affect the splitting strongly. However, the simple inverse relation between the splitting and the distance to the closest chaotic level (which also translates into a function of λ) as embodied in equation (9) will be modified. Nevertheless, even though one does not generally expect all the chaotic levels to move with exactly the same slope, locally over small λ-intervals, qualitatively similar behaviour to the three-level model as a function of λ still often holds.

It may seem odd at first encounter that coupling to chaotic levels could enhance tunnelling. After all, attempts are sometimes made to model coupling to the environment by coupling to chaotic degrees of freedom [10]. Under most circumstances, the environment quenches tunnelling [11]. In the limit of high density of chaotic levels with many lying close to the localized tunnelling pair, the three-level model must be expanded to incorporate a large number of strongly coupled, chaotic states (the coupling is strong because of the proximity of the levels, not an increase of the $\{v_{t,i}\}$). The requirement for tunnelling to take place, that one of the eigenstates must be either $|\pm\rangle$, is replaced by the notion that the full space can be subdivided into two subspaces each spanned by non-overlapping subsets of the true eigenvectors and that the projection of $|+\rangle$ into one of the two subsets must be unity and the projection of $|-\rangle$ must be unity into the other subspace. Equation (6) retains its same form except that the summation is extended to cover the larger space. It becomes highly improbable to satisfy the projection requirement and $\mathcal{P}$ approaches zero. Even if

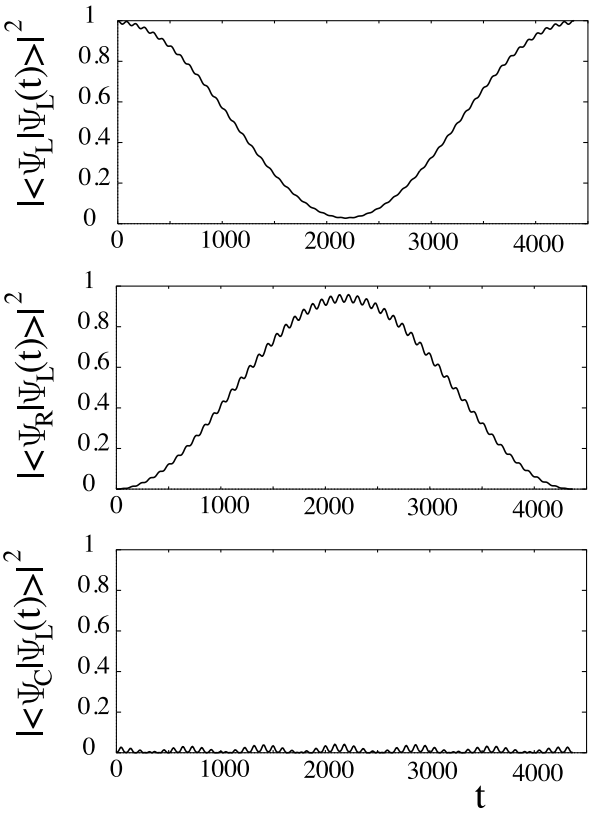

Figure 8. Time correlation functions of Ψ_L from figure 6.

some parameter range can be found which gives $\mathcal{P}$ approaching unity, the tunnelling time will be incredibly long due to the introduction of multiple, irrationally related timescales, all of which must lead simultaneously to certain combinations of phase shift relationships. In the strongly coupled limit, the image is thus one in which the symmetry breaking quenches the tunnelling and indirect interactions via the chaotic levels are insufficient to restore it.

In summary, we have shown how chaos-assisted tunnelling in a mixed phase space system lacking symmetry can be re-established through the variation of two external parameters. One parameter moves the two localized levels through an avoided crossing and the other moves the neighbouring delocalized or chaotic levels. If changes in the proximity of such 'third party' levels not involved in the avoided crossing itself strongly alters the minimum energy gap, the tunnelling is not via direct coupling. The parameter regimes are very narrow and require searching to locate them. Some of the tunnelling doublets couple most strongly to a single closest chaotic level. In these cases, the generalized three-level model expressed in equation (1) captures the essence of the tunnelling behaviour. A striking feature is the relationship expressed in equation (9) fixing the tunnelling times and localized level splittings by the avoided crossings between the regular and chaotic states. It was well satisfied for the quartic oscillator examples shown involving quantized tori and cantori. It was also possible to create extremely well-localized states from linear superpositions of just three eigenstates vindicating the basis of the given asymmetric three-level model. Other examples not shown required coupling to multiple chaotic levels rendering the signature

of chaos-assisted tunnelling less clean for them. We had quantum mechanics in mind throughout this paper, but the same considerations apply to other wave equations. With the results contained herein, several acoustic, microwave, and optical systems are imaginable that would display chaos-assisted tunnelling even though they may lack intrinsic symmetries (assuming their cavity Q-values can be made sufficiently high). As a final remark, we note that it would be very interesting to carry out an investigation of broken or absent symmetry and tunnelling behaviour between chaotic states [3] in a similar vein as this study of chaos-assisted tunnelling.

Acknowledgments

We gratefully acknowledge discussions with Denis Ullmo (also help with figure 2 and a critical reading of the manuscript) and Stephen Creagh, and support by the National Science Foundation under grant no PHY-9800106. We also gratefully acknowledge the support of E J Heller and ITAMP where much of the work was carried out.

References

[1] Bohigas O, Tomsovic S and Ullmo D 1993 *Phys. Rep.* **223** 43
Tomsovic S and Ullmo D 1994 *Phys. Rev.* E **50** 145
[2] Bohigas O, Boose D, Egydio de Carvalho R and Marvulle V 1993 *Nucl. Phys.* A **560** 197
Frischat S D and Doron E 1998 *Phys. Rev.* E **57** 1421
Lin W A and Ballentine L E 1990 *Phys. Rev. Lett.* **65** 2927
[3] Creagh S C and Whelan N D 1996 *Phys. Rev. Lett.* **77** 4975
For a review of dynamics and tunnelling see Creagh S C 1998 Tunneling in two degrees of freedom *Tunneling in Complex Systems* ed S Tomsovic (Singapore: World Scientific)
[4] Casati G, Graham R, Guarneri I and Izrailev F M 1994 *Phys. Lett.* A **190** 159
[5] Zakrzewski J, Delande D and Buchleitner A 1998 *Phys. Rev.* E **57** 1458
[6] Nöckel J U and Stone A D 1997 *Nature* **385** 45
[7] Heller E J, Stechel E B and Davis M J 1980 *J. Chem. Phys.* **73** 4720
Davis M J and Heller E J 1981 *J. Chem. Phys.* **75** 246
[8] Leyvraz F and Ullmo D 1996 *J. Phys. A: Math. Gen.* **29** 2529
See also Frischat S D and Doron E in [2]
[9] Shirts R B and Reinhardt W P 1981 *J. Chem. Phys.* **77** 5204
[10] See e.g. Jarzynski C 1995 *Phys. Rev. Lett.* **74** 2937
[11] Caldeira A O and Leggett A J 1983 *Ann. Phys.* **149** 374